Long-Range Coupling in an Allosteric Receptor Revealed by Mutant Cycle Analysis

Kristin R. Gleitsman,[†] Jai A. P. Shanata,[†] Shawnalea J. Frazier,[‡] Henry A. Lester,[‡] and Dennis A. Dougherty[†*]

[†]Divisions of Chemistry and Chemical Engineering and [‡]Biology, California Institute of Technology, Pasadena, California 91125

ABSTRACT The functional coupling of residues that are far apart in space is the quintessential property of allosteric proteins. For example, in Cys-loop receptors, the gating of an intrinsic ion channel is allosterically regulated by the binding of small molecule neurotransmitters 50–60 Å from the channel gate. Some residues near the binding site must have as their primary function the communication of the binding event to the gating region. These gating pathway residues are essential to function, but their identification and characterization can be challenging. This work introduces a simple strategy, derived from mutant cycle analysis, for identifying gating pathway residues using macroscopic measurements alone. In the exemplar Cys-loop receptor, the nicotinic acetylcholine receptor, a well-characterized reporter mutation (βL9′S) known to impact gating, was combined with mutations of target residues in the ligand-binding domain hypothesized or previously found to be functionally significant. A mutant cycle analysis of the macroscopic EC_{50} measurements can then provide insights into the role of the target residue. This new method, elucidating long-range functional coupling in allosteric receptors, can be applied to several reporter mutations in a wide variety of receptors to identify previously characterized and novel mutations that impact the gating pathway. We support our interpretation of macroscopic data with single-channel studies. Elucidating long-range functional coupling in allosteric receptors should be broadly applicable to determining functional roles of residues in allosteric receptors.

INTRODUCTION

Cys-loop receptors mediate fast synaptic transmission throughout the central and peripheral nervous systems (1–4). These pentameric, ligand-gated ion channels are prototypical allosteric receptors (5), in that the activation (gating) of an intrinsic ion channel is allosterically regulated by the binding of small molecule neurotransmitters (acetylcholine (ACh), serotonin, GABA, or glycine). Although valuable structural insights for Cys-loop receptors have appeared in recent years (6,7), detailed conformational mechanisms linking neurotransmitter binding to channel gating remain elusive.

Structurally, Cys-loop receptors have two principal functional domains (Fig. 1). The extracellular domain, rich in β-sheet structure, contains the agonist binding sites. Each subunit also contains a transmembrane domain comprised of four membrane-spanning helices, one of which (M2) lines the ion channel. Although the precise location of the channel gate has been debated, the consensus positions it at or below the middle of the M2 helix. This puts the channel gate 50–60 Å away from the agonist binding sites. Neurotransmitter binding events must therefore be communicated over this distance to the channel gate.

In terms of function, such a clear demarcation of domains is less evident. For a given residue, if a mutation at the site leads to a change in receptor function, this could be because the binding of agonist or the gating of the channel (or both) has changed. It seems safe to say that residues in the middle of the transmembrane domain do not contribute directly to agonist binding, and so residues in the transmembrane domain that contribute to function are typically described as ''gating'' residues. In contrast, one expects to find residues in the extracellular domain with varying functional roles. Some residues will primarily facilitate agonist binding, either by directly contacting the agonist or by refining the shape or electronic properties of the agonist binding site. However, to achieve the long-range communication that is fundamental to Cys-loop receptor function, other extracellular domain residues must be involved in communicating the binding event to the channel gate, serving an instrumental role in the gating pathway. These gating pathway residues are in some ways the most interesting, but their identification and characterization can be challenging.

One strategy for determining whether a given residue primarily contributes to agonist binding or channel gating involves single-channel recording on appropriate mutants, followed by kinetic analysis. However, in some Cys-loop receptors (such as 5-HT_3 (8)), single-channel conductances are too small for reliable kinetic analyses (9,10); in many other Cys-loop receptors, single-channel kinetics are complex or nonstationary, again vitiating single-channel kinetic analysis (11,12). Also, in other ion channels (13) and in allosteric receptors in general, single-channel studies are often not possible.

A more broadly applicable approach, allowing one to efficiently evaluate a number of mutants in search of unusual behavior, is to measure macroscopic currents across multiple concentrations. This produces the EC_{50} value, the

Submitted September 18, 2008, and accepted for publication December 15, 2008.

K. Gleitsman and J. A. P. Shanata contributed equally to this work.

*Correspondence: dadougherty@caltech.edu

Editor: David S. Weiss.

0006-3495/09/04/3168/11 $2.00

doi: 10.1016/j.bpj.2008.12.3949

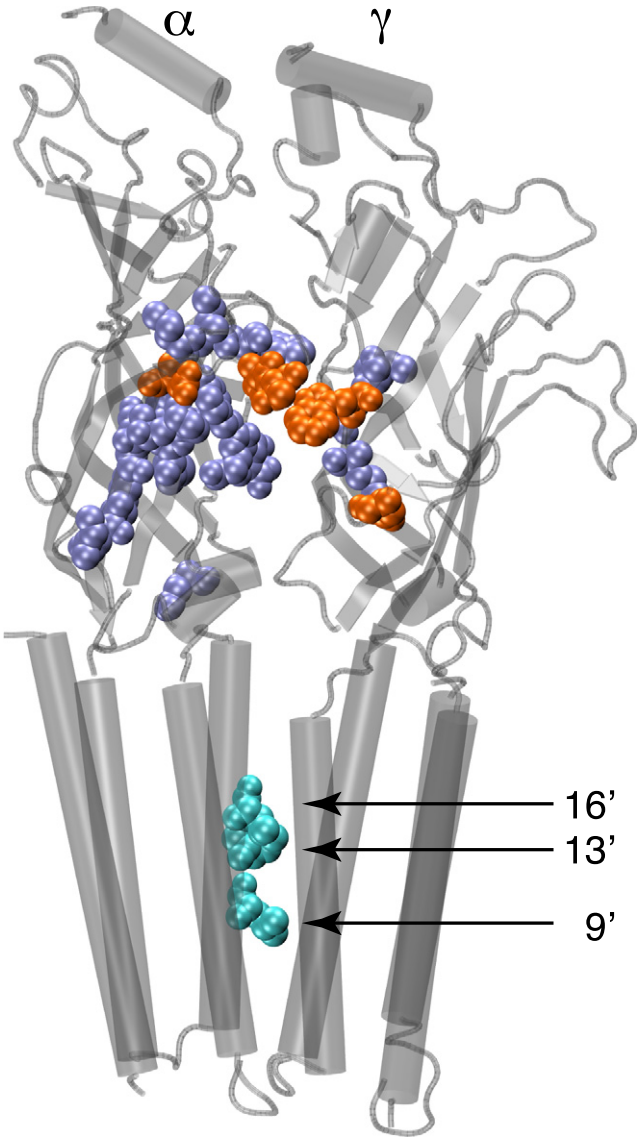

FIGURE 1 Residues considered here. Shown are two adjacent subunits of the cryo-EM structure of the *Torpedo* nAChR (pdb 2BG9) (7). The reporter residues in the transmembrane domain are shown as cyan and are labeled. Residues in the extracellular domain are in two classes: those with no long-range coupling (*purple*), and the five residues that show significant long-range coupling (*orange*). One noncoupling residue (γE168) is not defined in the EM structure and so is not shown.

concentration that induces half-maximal current in response to applied agonist, along with comparative measurements of maximal agonist-induced currents. In the case of ligand-gated ion channels, EC_{50} is a composite value, being responsive to both changes in agonist binding and channel gating behaviors. As such, it can be challenging to interpret shifts in EC_{50}. Here we describe an approach to use the readily obtained EC_{50} values to identify residues that substantially impact receptor gating. We refer to the method as ELFCAR (elucidating long-range functional coupling of allosteric receptors). The basic tool involves mutant cycle analysis of EC_{50} values for distant pairs of mutation sites. Complementary observations concerning mutational effects on receptor efficacy and the effects of partial agonists (PAs) support the basic methodology. Thus, ELFCAR provides an efficient strategy for identification of key gating pathway residues that may otherwise evade detection, without performing single-channel studies.

Key to the approach is the definitive feature of allosteric proteins: action at a distance. When a mutation in the transmembrane domain that is unambiguously associated with channel gating is paired with various mutations in the extracellular domain, the observation of nonmultiplicative EC_{50} shifts for the two mutations signals a functional coupling between the two residues, and thus identifies the extracellular domain mutation as influencing gating. We show that this behavior derives from the typical allosteric kinetic scheme for Cys-loop receptors, suggesting the approach could provide a general probe of allosteric receptors.

METHODS

Site-directed mutagenesis

Fetal mouse muscle nicotinic ACh receptor (nAChR) α-, β-, γ-, δ-subunits were utilized in the experiments. Each subunit was expressed in pAMV vectors. Mutations were made at the site of interest using a standard Stratagene QuikChange protocol. For the incorporation of unnatural residues, the site of interest was mutated to the amber stop codon. In addition, the α-subunits contain an HA epitope in the M3-M4 cytoplasmic loop for Western blot studies. Control experiments show that this epitope does not detectably alter EC_{50}. Primers were designed to fulfill the established criteria and were ordered from integral DNA technologies. Polymerase chain reaction (PCR) reactions were carried out using a high-fidelity Pfu DNA polymerase, and a 10 min extension time was used in each thermocycle. Annealing temperatures were modified as required for successful incorporation of the mutation. DpN1 digestion was used to eliminate methylated template DNA from the PCR products. After PCR purification (Qiagen standard protocol), amplification of the PCR product was conducted by electroporation with Super Competent Top 10 *Escherichia coli* followed by 12 h of growth on agar/Luria broth/ampicillin plates. Single colonies were selected and amplified in liquid Luria broth/ampicillin culture. The DNA was isolated from the bacteria (Qiagen, miniprep kit) and sequenced to verify the successful incorporation of the mutation at the selected site.

The circular bacterial plasmid of the mutation-containing DNA was linearized using a Not1 restriction enzyme. Linearized plasmids were used as the DNA template for in vitro transcription using T7 mMessage mMachine enzyme kits (Ambion) to make mRNA. Quantification of mRNA was determined using a NanoDrop spectrophotometer (NanoDrop Technologies, Thermo Scientific, Wilmington, DE).

For conventional mutations, the stoichiometry of subunits was 2:1:1:1 of α/β/γ/δ by mass with a total mRNA concentration of ~2 μg/μL. For unnatural mutations (14), a total of 40 ng of mRNA in a 10:1:1:1 α/β/γ/δ-subunit was coinjected with the synthetic α-hydroxy acids conjugated to the dinucleotide dCA and ligated to truncated 74-nucleotide tRNA as previously described. mRNA/tRNA were typically 1:1.

Stage V–VI oocytes of *Xenopus laevis* (Nasco, Fort Atkinson, WI) were injected with 50 nL of the mRNA or mRNA/tRNA mixture. The oocytes were incubated in culture media containing 1–2% horse serum at 18°C.

Whole-cell electrophysiology

Whole-cell electrophysiological recordings were performed on injected *Xenopus laevis* oocytes after 12–36 h incubation. Recording was done in two-electrode voltage clamp mode using the OpusXpress 6000A (Axon

Instruments, Union City, CA). Oocytes were superfused with Ca^{2+}-free ND96 solution (in mM: 96 NaCl, 2 KCl, 1 $MgCl_2$, 5 HEPES) at flow rates of 4 mL/min during drug application (15 s) and 3 mL/min during wash (130 s). Macroscopic agonist-induced currents were recorded in response to bath application of the indicated agonist concentrations at −60 mV or −80 mV. Data were sampled at 125 Hz and filtered at 50 Hz. ACh chloride and succinylcholine (SuCh) chloride were purchased from Sigma/Aldrich/RBI (St. Louis, MO). Agonist solutions ranging from 0.0100 μM to 5000 μM were prepared in Ca^{2+}-free ND96 from a 1 M stock solution. Dose-response relations were constructed for each mutation using data from ≥5 oocytes. Dose-response relations were fitted to the Hill equation (Eq. 1) to determine the EC_{50} and the Hill coefficient:

$$I/I_{max} = 1/(1 + (EC_{50}/[A])^{n_H}), \quad (1)$$

where I is the current for agonist concentration [A], I_{max} is the maximum current, EC_{50} is the concentration to elicit half maximal response, and n_H is the Hill coefficient. The dose-response relations of individual oocytes were examined and used to determine outliers. The reported EC_{50} values are from the curve fit of the averaged data.

Single-channel characterization of selected gating pathway residue mutants

Single-channel recording was performed in the cell-attached configuration on devitellinized oocytes 24–60 h after injection at 20 ± 3°C with an applied pipette potential of +100 mV, as described previously (15). Pipettes were fabricated from thick-walled (inner diameter = 0.80 mm, outer diameter = 1.60 mm) KG-33 glass (Garner Glass, Claremont, CA) and coated with Sylgard (World Precision Instruments, Sarasota, FL); they had resistances of 8–25 MΩ. The bath solution contained, in mM, 120 KCl, 5 HEPES, 1 $MgCl_2$, 2 $CaCl_2$, pH = 7.4, so that the transmembrane potential of the patch was −100 mV, and the reversal potential for agonist-induced currents was ~0 mV. The pipette solution contained, in mM, 100 KCl, 10 HEPES, 1 $MgCl_2$, 10 K_2EGTA, pH = 7.4 and was supplemented with the indicated concentrations of ACh using a 1 M stock solution.

Before single-channel recording, whole-cell expression levels were determined with 100–1000 μM ACh doses using the whole-cell recording conditions on each mutant. When whole-cell expression exceeded ~300 nA for receptors with the target mutation alone and ~3 μA for receptors with a target mutation and a reporter mutation, oocytes were typically incubated 4–10 additional h before single-channel recording. Data were collected using a GeneClamp 500B amplifier (Axon Instruments, Union City, CA) with a CV-5 100 GU headstage at full bandwidth (4-pole Bessel, −3 dB, 50 kHz). The signal was then low-pass filtered (8-pole Bessel, −3 dB, 20 kHz) and sampled with a Digidata 1320A and Clampex 9.2 (Axon Instruments, Union City, CA) at 50 or 100 kHz. Only recordings that showed no simultaneous activations were included in NP_{open} analysis. In this manner, ≥three patches at EC_{50} were analyzed for all mutants, except for the $\alpha\beta\gamma$D174NδD180N and $\alpha\beta$L9′S γD174NδD180N mutants for which two patches each were obtained. Data were filtered offline (Gaussian, −3 dB, 5 kHz) and electrical interference at harmonics of 60 Hz was removed, if necessary. Event transitions were detected with Clampfit 9.2 (single-channel search). A dead time, t_d, of 40 μs was applied to all events. The time-average probability that exactly one channel in the patch is open (NP_{open}) was calculated as the total open time divided by the sum of the total open time and the total closed time.

RESULTS

The prototypical and most-studied Cys-loop receptor, the muscle nicotinic ACh receptor (nAChR), was used in this study. It is important to appreciate that the method is directly applicable to other Cys-loop receptors, and, in favorable cases, to other allosteric proteins as well. Here we have employed the muscle-type nAChR as a well-established system that allows us to evaluate the methodology.

The muscle nAChR is a heteropentamer with subunit composition $(\alpha 1)_2\beta 1\gamma\delta$. Two nonequivalent binding sites are located in the extracellular domain at the $\alpha-\delta$ and $\alpha-\gamma$-subunit interfaces. Nearly all Cys-loop receptors, including all nAChRs, contain a conserved leucine residue in the hydrophobic, pore-lining M2 helix of each subunit (Fig. 1). Mutating this residue, termed L9′, to serine lowers the EC_{50} (16,17). Structural studies place L9′ near the middle of the M2 helix, in the region of the occlusion of the closed channel, and although it can be debated whether L9′ constitutes a literal gate of the channel, there can be no doubt that it is a crucial gating residue. In this work, the L9′S mutation in the β-subunit was used as a reporter to evaluate mutations of residues in the extracellular domain that may function as binding residues or as gating pathway residues.

βL9′S as a reporter of functional role for extracellular residues

Agonist occupancy at both binding sites is required for efficient opening of the channel pore. Scheme 1 shows a simplified kinetic model for activating the nAChR, leading to an expression for EC_{50} (Eq. 2) (18,19), where A is the agonist; R^C and R^O denote the closed and open states of the receptor; k_1 and k_{-1} are forward and reverse rate constants for agonist binding; K_D is the dissociation constant for the agonist; and Θ is the gating equilibrium constant, given by the ratio of the channel opening rate, β, to the channel closing rate, α. It is well understood that the actual kinetic model for the nAChR is likely more complicated, and that different Cys-loop receptors may show kinetic schemes that differ in detail. In addition, a strong gating mutation could enable spontaneous openings of the channel when no agonist is bound. This could compromise the kinetic model discussed here. However, the βL9′S mutation alone does not lead to extensive spontaneous openings, and the types of mutations emphasized here, if they impact gating at all, discourage channel opening (decrease Θ), suggesting that spontaneous openings will not produce a major perturbation to the system. Scheme 1 is typical for an allosteric receptor, capturing the essence of the situation: function depends on binding of an allosteric effector as well as signal transduction (gating). For ligand-gated ion channels, this means that EC_{50} depends on K_D and Θ, where Θ is a measure of receptor efficacy. The graphical representation of the relationship between EC_{50} and Θ, based on Eq. 2, is shown in Fig. 2. Simulations of more-complex kinetic schemes produce qualitatively similar plots. For full agonists (FAs), that is, those that produce a large Θ, the plot is linear with a negative slope. We will refer to this as the ''high slope'' region of the plot. For smaller values of Θ, such as would be associated with partial agonism, the plot approaches an asymptote. We will refer to this as the ''plateau'' region:

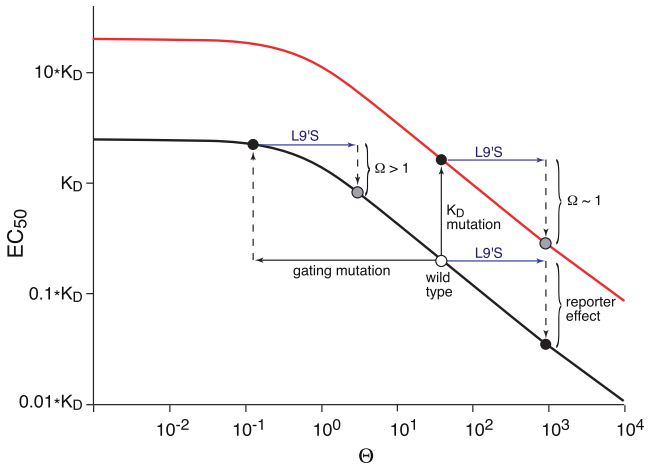

FIGURE 2 (*Black line*) Relationship between EC_{50} and Θ, as given in Eq. 2. (*Red line*) The same equation but with a larger K_D. For both plots, in the negative slope region changes in Θ produce significant changes in EC_{50}, as shown when the reporter effect is added to the wild-type receptor. However, when beginning with Θ in the plateau region, a much smaller shift in EC_{50} occurs for equivalent shifts in Θ.

$$A + R^C \underset{k_{-1}}{\overset{2k_1}{\rightleftarrows}} A + AR^C \underset{2k_{-1}}{\overset{k_1}{\rightleftarrows}} A_2R^C \underset{\alpha}{\overset{\beta}{\rightleftarrows}} A_2R^O, \quad \text{Scheme 1}$$

where $K_D = k_{-1}/k_1$ and $\Theta = \beta/\alpha$

$$EC_{50} = \frac{K_D}{(\Theta + 2)^{1/2} - 1}. \quad (2)$$

A defining feature of allosteric proteins is that an allosteric effector shifts the equilibrium between two states, historically termed tensed and relaxed. However, binding of the allosteric effector itself does not define the exact state as tensed or relaxed, rather it produces a shift in the equilibrium distribution between these states. Consequently, once the allosteric signal is saturated, this equilibrium distribution depends only on the equilibrium constant governing tensed-relaxed interconversion. In the case of ligand-gated ion channels, such as the nAChR studied here, different allosteric effectors—i.e., different ligands for ligand-gated ion channels—produce different closed-open equilibria, characterized by Θ. Thus, whereas FAs ($\Theta >> 1$) cause the channel to be mostly open when agonist is bound, PAs influence this allosteric transition to a lesser extent, resulting in a smaller perturbation of the gating equilibrium. It is the varying extent to which ligand binding can bias the equilibrium that produces the general shape of the relationship between EC_{50} (function) and Θ, seen in Fig. 2.

Previous studies (17,20–22) have shown that polar mutations at L9′ substantially increase Θ, causing a corresponding drop in EC_{50}. Our goal was to determine whether it was possible to use a reporter mutation such as βL9′S to evaluate whether the shift in EC_{50} from mutation at a target residue is primarily a result of changes in binding (K_D) or gating (Θ) (see the Supporting Material, Fig. S1). Consider such a target mutation in the extracellular domain that only increases K_D, i.e., a pure binding mutation. This has the effect of raising the EC_{50} versus Θ curve, but maintaining its shape (Fig. 2, *red line*). Addition of the βL9′S mutation then causes a comparable increase in Θ, lowering EC_{50} by the same factor as in the wild-type. The pairing of an extracellular domain binding mutation with the reporter transmembrane domain mutation results in a multiplicative shift in EC_{50}; the two mutations are independent.

Now, consider the consequences of an extracellular domain target mutation that affects gating, and not binding. Deleterious mutations (increase in EC_{50}) will cause a drop in Θ, and if the effect is large enough, the agonist employed will now be a PA. The EC_{50} versus Θ relationship for this mutant will now lie in the plateau region of Fig. 2. As a result, the subsequent increase in Θ caused by adding the βL9′S mutation will induce a much smaller drop in EC_{50}. The pairing of these mutations will no longer give a multiplicative shift in EC_{50}, and therefore the two mutations are functionally coupled. Thus, the βL9′S gating mutation acts as a reporter to identify a target mutation that is substantially loss of function (decreasing Θ). It is clear from Fig. 2 that a gain-of-function gating mutation (lower EC_{50}; increasing Θ) will still be in the high slope region and so will be additive with the βL9′S mutation. This method cannot detect gain-of-function gating mutations.

For many mutations in the extracellular domain, the βL9′S mutation is multiplicative, producing a consistent 40-fold shift to lower EC_{50} (Table 1) (17,23,24). We now report the first examples of mutations closely associated with the agonist binding site for which the effect of βL9′S is substantially <40-fold, indicating nonmultiplicative behavior (Fig. 1). Four of these are conventional mutants: αY190F, γD174NδD180N, γW55YδW57Y, and αD200N. Others have probed these sites, and they are generally considered to primarily influence gating (25–31). As such, these studies validate the ELFCAR method. The fifth, a novel mutant, replaces αS191 with its α-hydroxy analog, which we abbreviate Sah (for serine α-hydroxy), converting the backbone amide that links αY190 and αS191 to a backbone ester (32,33).

Mutant cycle analysis suggests long-range coupling

The typical way to analyze a system in which two mutations are evaluated, individually and in tandem, is by mutant cycle analysis (Fig. 3). Briefly, if a mutation at one site has no structural or energetic impact at a second site, then the effect of simultaneous mutations at both sites will simply be multiplicative (Fig. 3). In the parlance of mutant cycle analysis, the coupling parameter, Ω, will be unity. In contrast, if two residues interact, the simultaneous mutation at both sites will lead to an effect that is either greater or less than the product of their individual effects, producing an Ω-value

TABLE 1 EC_{50} values with and without βL9′S reporter mutation for coupled and noncoupled residues

Target mutation	WT EC_{50}	EC_{50} with reporter mutation	Ratio	Ω
		βL9′S		
Wild-type	46	1.2	38	1.00
γD174Nδ D180N	590	160	3.7	11
αY190F	1200	520	2.3	17
γW55Yδ W57Y	180	24	7.5	5.1
αD200N	130	29	4.5	8.6
αS191Sah	300	50	6.0	6.4
αE45W	120	3	40	0.96
αY93Yah	39	1	39	0.98
αN94Nah	87	2.2	40	0.97
αD97E	3.3	0.09	37	1.0
αM144L	15	0.37	41	0.95
αM144Lah	50.4	1.3	39	0.99
αK145Q	170	8.1	21	1.8
αL146Lah	26	0.5*	52	0.74
αT148Tah	33	1.3	25	1.5
αW149Wah	36	0.72	50	0.77
αW149 5-F-Trp	200	4.7	43	0.90
αW149 5-Br-Trp	88	2	44	0.87
αL199Lah	11	0.18	61	0.63
αT202Tah	24	0.48	50	0.77
αY203Yah	39	0.62	63	0.61
αF205Yah	67	1.4	48	0.80
αF205Y	90	1.5	60	0.64
αV206Vah	170	3.1	55	0.70
γL36δ L39Lah	28	0.63	44	0.86
γI56δ I58Iah	33	0.83	40	0.96
γA121δ A124Aah	25	0.66	38	1.0
γE168Qδ E175Q	42	1.2	35	1.1
		γL9′S		
Wild-type	46	4.5	10	1.0
γD174Nδ D180N	590	244	2	4.2
αY190F	1200	650	2	5.5
γW55Yδ W57Y	180	74	2	4.2
		δL9′S		
Wild-type	46	1	46	1.0
γD174Nδ D180N	590	140	4	11
αY190F	1200	370	3	14
γW55Yδ W57Y	180	16	11	4.1
		αL9′S		
Wild-type	46	0.35	131	1.0
γD174Nδ D180N	590	65	9	14
αY190F	1200	223	5	24
γW55Yδ W57Y	180	7.5	24	5.5
		αV13′S		
Wild-type	46	0.1	460	1.0
γD174Nδ D180N	590	8.9	66	7
αY190F	1200	32	38	12
γW55Yδ W57Y	180	1.5	120	3.8
		αL16′S		
Wild-type	46	0.47	98	1.0
γD174Nδ D180N	590	59	10	10
αY190F	1200	190	6	15
γW55Yδ W57Y	180	8.5	21	4.6

Values for the three coupled residues are also given for reporter mutations in all other subunits (γ, δ, and α) and positions (9′, 13′, and 16′). The ratio of EC_{50}s: target/target with reporter, and resultant calculated Ω-values are also reported. The standard error for all EC_{50} values was <10%, except for *, which had standard error of 20%. Data at sites α148(51), α149(24), and αS191(47) have been reported previously.

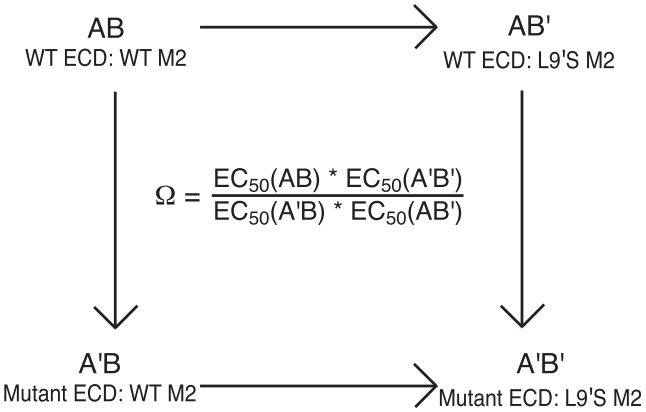

FIGURE 3 Scheme for double mutant cycle analysis where *A* and *B* represent amino acid positions and *A′* and *B′* represent mutations at these sites. The coupling parameter, Ω, is calculated from the given equation.

that significantly deviates from unity. This approach has been broadly applied to a wide range of systems, including Cys-loop receptors, where several investigators have used mutant cycle analysis of EC_{50} values to determine functional coupling between neighboring residues of the extracellular domain (34–36).

As could be anticipated from the EC_{50} values in Table 1, the majority of mutations made in the extracellular domain of the nAChR produce an Ω for coupling to βL9′S of ~1, indicating the functional independence of these residues. However, the five mutations noted above—αY190F, γD174Nδ D180N, γW55Yδ W57Y, αD200N, and αS191Sah—produced larger Ω-values. We consider a value of $\Omega > 2$ to signify a meaningful coupling (Fig. 4). Phenomenologically, this establishes a long-range coupling between these extracellular domain sites and the βL9′ site, as one would expect for an allosteric receptor. Typically, an Ω that deviates significantly from a value of 1 is interpreted to indicate a direct interaction between the residues, such as a hydrogen bond or a salt bridge. In this work, though, such a direct interaction is clearly impossible. We feel the interpretation of Fig. 2 is much more palatable. Significant coupling is seen because both the βL9′S mutation and the particular extracellular domain mutation disrupt the gating pathway.

Single-channel recording supports whole-cell mutant cycle analysis conclusions

The most convincing way to evaluate the impact of a particularly interesting mutation is by single-channel analysis. To test our interpretation of the mutant cycle analyses using EC_{50} values, we chose three extracellular domain mutants that ELFCAR identified as gating pathway residues (αY190F, γD174Nδ D180N, and γW55Yδ W57Y) for single-channel studies. From these recordings, the open probability in the patch, NP_{open} was obtained. *N* is the number of channels in the patch, which often cannot be precisely determined. P_{open} is derived from Scheme 1 and

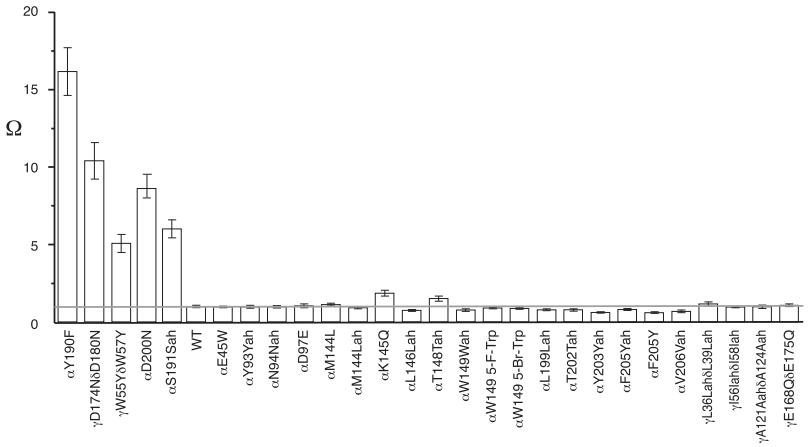

FIGURE 4 Values of Ω (coupling to βL9′S) for mutations considered here. The standard 40-fold shift expected for a βL9′S mutation produces an Ω-value of one (*horizontal line*). 5-F-Trp is 5-fluorotryptophan and 5-Br-Trp is 5-bromotryptophan. For α-hydroxy acids (Yah, Nah, Lah, Tah, Wah, Vah, Iah, and Aah), a three-letter abbreviation is used: the one-letter code for the parent amino acid is followed by ah; thus Yah is the α-hydroxy acid of tyrosine.

depends only on Θ at equivalent points on the dose-response relation. The NP_{open} measurements reported were obtained using the macroscopic EC_{50} concentration of ACh, and thus represent $0.5(NP_{open,max})$. Each of the three target mutations produces a large decrease in NP_{open} (Fig. 5; Table 2) compared to the wild-type value of ~0.5 (data not shown); they are substantially deleterious gating pathway mutations. Also consistent with the model, adding the βL9′S mutation substantially increases NP_{open}. The single-channel analysis thus supports the interpretation of the macroscopic EC_{50} data.

Other reporter mutations support gating pathway assignments

An implication of this experimental strategy is that other residues in the transmembrane domain that substantially increase Θ could act as reporters for extracellular domain residues; we are not limited to the β-subunit or the well-characterized L9′ position. To test this notion, L9′S mutations were made in the α-, γ-, and δ-subunits, and two other Ser mutations were made in the M2 helix of the α-subunit at positions V13′ and L16′ (Fig. 1). All of these mutations lower EC_{50} significantly, and all positions are confidently ascribed to be gating residues. As shown in Fig. 6, the extracellular domain mutations that give significant Ω-values with βL9′S also show significant Ω-values with L9′S mutations present in the other subunits. Recalling that there are two α-subunits, we find a general coupling parameter sequence of $\beta \approx \delta > \alpha > \gamma$. Thus, subtle asymmetries between subunits exist regarding the L9′ residues' contribution to gating, which are also reflected in the EC_{50} values of the various L9′S mutants (Table 1). If one considers positions other than 9′, all the mutated gating pathway residues again produce meaningful Ω-values, and the magnitude of their effect is consistently $\alpha 9' > \alpha 16' > \alpha 13'$ (Fig. 6).

The reporter mutation βL9′S systematically increases I_{max} for gating pathway residues

This interpretation of the mutant cycle analysis data predicts other behaviors for extracellular gating pathway residues. For example, to produce a significant mutant cycle analysis coupling to L9′ (Ω >2), the mutation in the extracellular domain must convert ACh to a PA, such that the target mutation is now in the plateau region of Fig. 2. Due to this decrease in Θ, the maximal current observed in response to saturating concentrations of ACh (I_{max}) should diminish. In general, interpreting differences in I_{max} can be challenging due to variations in whole-cell current among oocytes, which can stem from various sources that may or may not relate to the actual mutation in question. However, use of a reporter mutation can assist in the interpretation of I_{max} differences. For mutations that render ACh a PA, increasing efficacy through a reporter mutation produces a significant systematic increase in I_{max} (Fig. S2). We find that these increases are larger and more consistent than the typical variability in I_{max} in conventional mutagenesis studies. Thus, if a receptor with a target mutation shows a large increase in mean I_{max} on introduction of a reporter mutation, the mutation likely affects gating. This is shown in Fig. 7 for mutations with large Ω-values, along with several examples with Ω near one. Recovery of I_{max} by introduction of the reporter mutation confirms the gating pathway residue assignments made by mutant cycle analysis. Moreover, the single-channel observations support this interpretation, in that the increase in NP_{open} is the microscopic correlate of the macroscopic observation of recovery of I_{max} (Table 2; the quantitative differences between Ω, I_{max}, and NP_{open} are considered in the Supporting Material).

Experiments with the PA SuCh support gating pathway assignments

Given the argument that a substantially deleterious mutation of a gating pathway residue converts the FA ACh to a PA, which manifests as a diminished I_{max}, it is interesting to consider the behavior of an inherent PA, such as SuCh (37). The relative efficacy, ε, of a PA can be defined as the ratio of the maximal current elicited by a PA to the maximal current elicited by a FA (Eq. 3). At saturating doses of

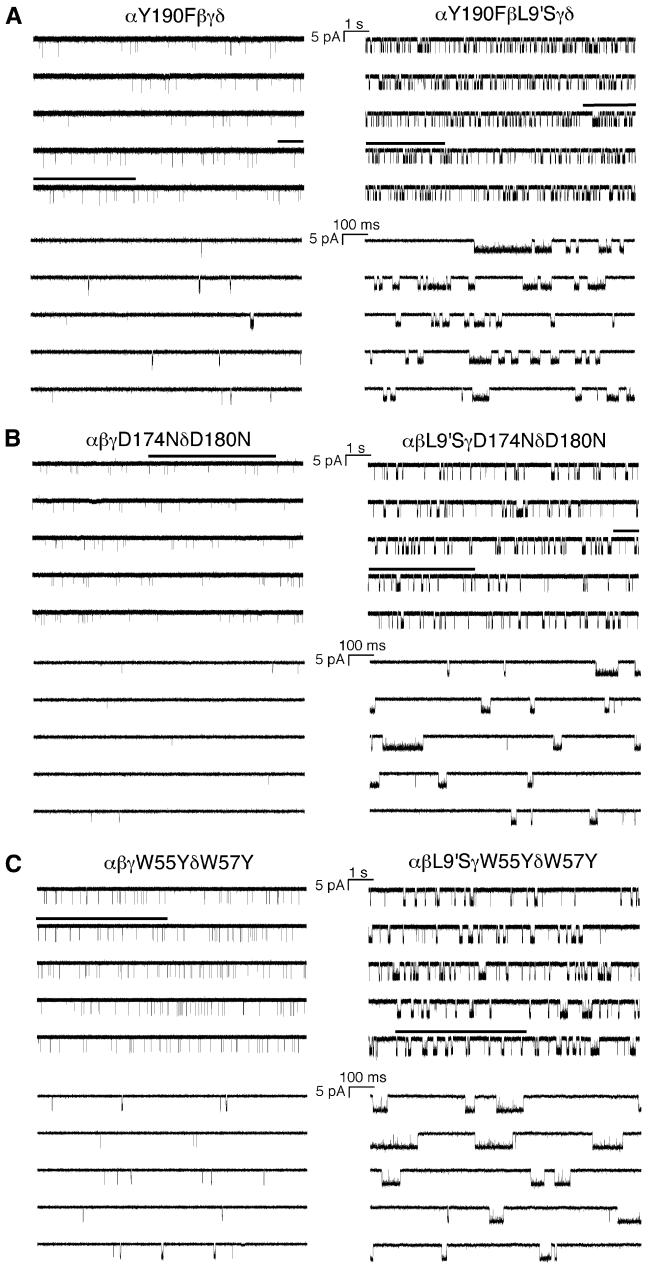

FIGURE 5 Single-channel currents for select mutants. In each case, ACh is applied at the macroscopic EC_{50} value (Table 1), and the left panel has no reporter mutation, whereas the right panel is for receptors with the βL9′S reporter mutation. For each of the six receptors, the lower trace (5 s) depicts an expansion of the section of the upper trace indicated with a line. Records were obtained in the cell-attached configuration with a pipette potential of +100 mV and are shown at 5 kHz bandwidth. Channel openings are shown as downward deflections. (*A*) αY190F; (*B*) γD174NδD180N; and (*C*) γW55YδW57Y.

agonist, all the receptors are presumed to be in a diliganded state (A_2R), meaning that differences in I_{max} for the two agonists are due to differences in the probability that a single channel is open when the binding equilibrium is saturated, $P_{open,max}$. For wild-type muscle nAChR, SuCh is a PA with ~4% efficacy relative to ACh.

TABLE 2 Coupling parameter, Ω, and I_{max} ratio from whole-cell data. NP_{open} values (mean ± SE) at respective macroscopic EC_{50} values (Table 1)

Mutant	Ω	I_{max} ratio	NP_{open}	NP_{open} βL9′S
αY190F	17	11	0.0026 ± 0.0006	0.18 ± 0.04
γD174NδD180N	11	13	0.0007 ± 0.0005	0.08 ± 0.06
γW55YδW57Y	5	12	0.018 ± 0.005	0.26 ± 0.06

$$\varepsilon = \frac{I_{max,PA}}{I_{max,FA}} = \frac{P_{open,max,PA}}{P_{open,max,FA}}, P_{open,max} = \frac{\beta}{\alpha + \beta} = \frac{\Theta}{\Theta + 1} \quad (3)$$

In the presence of an L9′S mutation alone, SuCh becomes a FA (see Fig. S3). Three of the five gating pathway residues were characterized using the PA SuCh. Unlike what is observed for binding mutations, when αY190F, γD174NδD180N, and γW55YδW57Y contained a $L \rightarrow S$ mutation at either the 9′ (α or β), 13′ (α), or 16′ (α) site, the recovery of SuCh toward full agonism is blocked. As before, the magnitude of the effect follows the trend $\alpha 9' > \alpha 16' > \alpha 13'$ (data not shown). This is interpreted as further evidence that mutation of these extracellular domain residues drastically impairs normal gating function. Note that the efficacies of SuCh for the gating pathway mutants without the L9′S reporter mutation are not dramatically different from that of wild-type (0.04 ± 0.02 for wild-type, 0.04 ± 0.01 for αY190F, 0.02 ± 0.01 for γD174NδD180N, and 0.01 ± 0.0009 for γW55YδW57Y). This again highlights how the use of a reporter mutation can uncover important aspects of receptor function that might otherwise be missed.

DISCUSSION

In this work, we propose that appropriately designed double mutant studies can provide valuable insights into the mechanism of action of an allosteric receptor. We begin with a mutation at a site whose function is unambiguous. Here, this reporter residue can be one of several sites in the transmembrane region of a ligand-gated ion channel, far removed

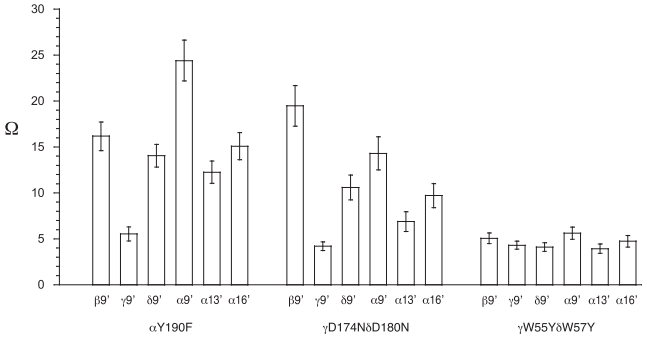

FIGURE 6 Values of Ω for various reporter mutations. For each of the three extracellular domain mutations, results for six different reporter mutations are shown. Reporter mutations are identified by their location, in each case, the mutation is of a hydrophobic residue to serine.

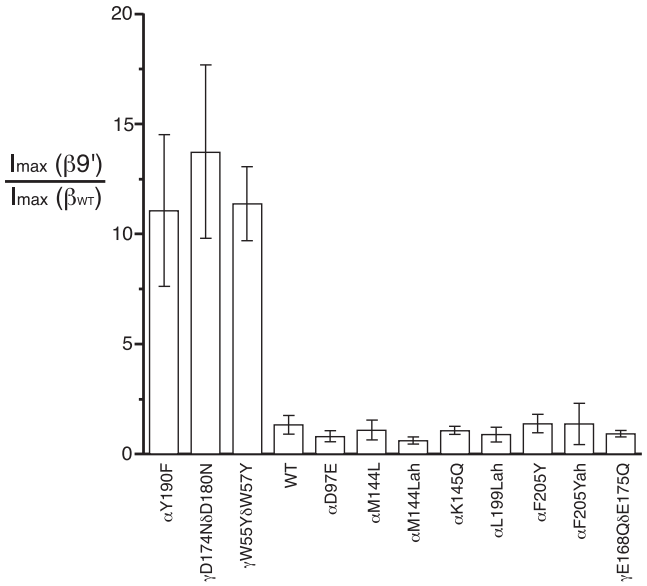

FIGURE 7 Variation in I_{max} in response to introduction of a βL9′S reporter mutation.

from the agonist binding site. It is assumed that mutations at this site primarily, if not exclusively, perturb the gating of the receptor, and this view is supported by detailed studies of the reporter mutations. A second site, the target site, can then be probed by combining mutations there with a reporter mutation. Here we consider a number of target sites that are far removed from the reporter residue. Analysis of the results can proceed along several lines. The classical tool is a mutant cycle analysis. Indeed we find that, whereas most pairings of remote residues produce independent behavior ($\Omega \sim 1$), for select target residues a mutant cycle analysis produces strong coupling parameters. Typically, such coupling is interpreted to indicate a direct interaction between the residues. However, in all cases here, the residues are much too far apart to accommodate a direct structural interaction. As such, we have an allosteric coupling between remote residues, which manifests in a mutant cycle analysis just as if the two were structurally coupled. Of course, such action at a distance is the definitive feature of an allosteric system, but there are few cases where such pairwise interactions have been seen. Because the reporter mutation influences gating, coupling requires that the target residue also impact gating, allowing an apparent long-range interaction to be revealed in the mutant cycle analysis. We have labeled such residues as being on the ''gating pathway'', with the understanding that any mutation that preferentially stabilizes one state of the receptor could produce a positive result in ELFCAR, regardless of its location in the receptor. The particular residues studied here, however, do lie in regions of the receptor that have been considered to be part of the primary structural transduction from binding site to channel gate.

A less-phenomenological analysis can be made with reference to Fig. 2. The key here is that if the mutation at the target site perturbs gating by decreasing Θ, moving the system to the left along the EC_{50} versus Θ curve, and, if the effect is large enough, the system will now be in the plateau region. Then, when the reporter mutation is added, its effect on EC_{50} will be diminished relative to what is seen in the receptor that is wild-type at the target site. To be informative, the mutation at the target site must be loss of function (diminished Θ) and must have a substantial effect on gating. If Θ is diminished only slightly by the target mutation, or if Θ is increased (gain of function) the system will remain in the region of high slope, and the reporter mutation will have its normal effect. Also, when we do see significant coupling, that does not rule out the possibility that K_D has changed in addition to Θ; ELFCAR can only establish that a significant decrease in Θ has occurred. At the same time, when a target mutation produces a large shift in EC_{50} but a conventional 40-fold additional shift on adding the βL9′S reporter mutation, it is tempting to conclude that the target mutation exclusively impacted K_D. However, changes in Θ that are significant but not large enough to move the system into the plateau region of Fig. 2 could be involved in addition to or instead of a K_D change. For example, the K145Q mutation has been reported to impact gating (28), but without moving Θ into the plateau region. In this work, K145Q shows a marginal functional coupling with L9′S, with an Ω-value near the cutoff for significance (1.8 ± 0.2). As such, ELFCAR is best suited to identifying mutations that strongly perturb gating ($\Omega > 2$); negative results should be interpreted cautiously. Note that in receptors for which the wild-type Θ is smaller than in the muscle-type nAChR, ELFCAR would be expected to be more sensitive to small changes in Θ.

Several additional observations support our analysis of the results seen here. First, in a typical mutant cycle analysis, Ω-values <1 can be observed and are functionally significant. However, in this context, the model of Fig. 2 allows only for $\Omega > 1$, which is consistent with our data. Importantly, three mutations shown here to impact gating by the ELFCAR approach have been confirmed to be gating mutations by single-channel analyses. The single-channel values we report are NP_{open}. The true probability that a single channel is open at these concentrations, P_{open}, is increased by a factor of N, where N is the number of channels in the patch. Because the measured probability that the channel is open is low ($\leq 2\%$) for the gating pathway mutations without the reporter mutation, the number of channels in the patch cannot be determined. However, if there are actually multiple channels in these patches, our NP_{open} values would be overestimates of P_{open}. The measured NP_{open} values are substantially diminished upon addition of each of the three target residues we tested (αY190F, γD174NδD180N, and γW55YδW57Y), such that the modest perturbation of EC_{50} associated with the target mutations can be primarily ascribed to dramatic changes in the gating pathway. Other single-channel studies of residues considered here are also consistent with our findings.

Other observations support our general model. If a target mutation substantially reduces Θ, then ACh should become a PA at the receptor. This should lead to reduced maximal currents from whole-cell recordings, and just such an effect is seen. Also, an inherent PA should be sensitive to the consequences of the target mutation, and we find that is the case for SuCh.

It is interesting to consider the residues that have been probed here; Fig. 1 highlights them all. The considerable distance between the reporter residues and the target residues is clear from this image. Concerning the target residues, those with no strong coupling (*purple*) are dispersed throughout the extracellular domain, and, although only five have been identified so far, the same is true of the gating pathway residues (*orange*). There is no simple pattern that distinguishes the two classes.

The agonist binding site of the nAChR is an ''aromatic box'', shaped by five conserved aromatic residues: αY93 (A), αW149 (B), αY190 (C1), αY198 (C2), and γW55/δW57 (D) (6,38). The letter designations signify the ''loop'' of the extracellular domain that contains the particular residue (39). Because all the natural agonists of Cys-loop receptors have a cationic group, the presence of the aromatic box suggested that a cation-π interaction contributes to agonist binding (40,41). Indeed, αW149 (B) and the aligning residues have been shown to contribute to agonist binding through a cation-π interaction in both the nAChR and the 5-HT_3 receptors (24,42). We find Ω ~ 1 consistent with a binding role for this residue. Note that subtle mutations have been employed at this site, taking advantage of the power of unnatural amino-acid mutagenesis. We cannot rule out the possibility that more disruptive mutations at this and other sites would impact receptor gating. Indeed, the αW149F mutation has been probed, and it impacts binding and gating (43). Most of the mutations in Table 1 are, by conventional standards, subtle, and we would argue that some caution must by employed in interpreting the consequences of more severe mutations.

The residue analogous to αY198 (C2) has been shown to bind serotonin through a cation-π interaction in the MOD-1 receptor (44). Previous studies in the nAChR show that mutations at this site exhibit normal coupling to L9′S mutations (45). Single-channel studies of the αY198F mutant indicate only modest changes in gating (26) that would be outside the limits of detection for ELFCAR.

The residue αY93 (A) has been extensively probed. In the $GABA_A$ receptor the analogous residue makes a cation-π binding interaction to the native agonist (46). In the nAChR, side-chain mutations at this site strongly impact channel gating. However, the mutation studied here, αY93Yah, is a backbone mutation. Our finding of Ω ~ 1 indicates no strong perturbation of gating by a backbone mutation in this region. This conclusion is supported by the similar result at the adjacent residue (αN94Nah).

The remaining two box residues, αY190 (C1) and γW55/δW57 (D), have never been shown to make a cation-π interaction with an agonist. Both are assigned as gating pathway residues according to the ELFCAR method. αY190 has been extensively studied. That αY190F strongly impacts gating is unambiguously established by the single-channel records of Fig. 5 *A*. Other workers have also found strong perturbations to gating for mutations at this site (27,28). Some studies have also found a contribution to binding, but, as discussed above, this work does not address this issue. The important point is that the finding of a large Ω-value in ELFCAR is supported by single-channel studies. In addition, a backbone mutation at the adjacent residue, αS191Sah, also produces a large Ω-value in ELFCAR. We have recently shown that this residue makes a strong hydrogen bond to a side chain from the complementary subunit (γ/δ) and that the hydrogen bond contributes significantly to gating (47). Most gating models for the nAChR invoke considerable movement of loop C (6,48,49), and the finding of large Ω-values for these two loop-C residues is consistent with these models.

The final binding box residue, γW55/δW57 (D), shows a large Ω-value for the Tyr mutant. Our single-channel studies (Fig. 5 *C*) establish an impact on gating for this mutation. Previous single-channel studies of the Phe mutant show a small effect on binding (3.4-fold) and a large effect on gating (50-fold) (50), consistent with these results. There is reason to anticipate that loop D may also undergo significant rearrangements during gating. In Unwin's image of the *Torpedo* nAChR (7), with no agonist bound, TrpD is flipped out away from the box that is so well formed in AChBP (with or without agonist bound). This again suggests that movement of TrpD occurs on ligand binding, consistent with it being a gating pathway residue.

The fifth gating pathway residue we identified, αD200, is not part of the aromatic binding box but appears to lie outside the box. However, it is part of a triad of residues that includes αY190 and αK145 and that has been suggested to undergo significant rearrangement on gating (28). Previous single-channel studies have shown that mutation at this site perturbs gating (25,28). As such, the large Ω seen here with ELFCAR is consistent with other studies.

CONCLUSIONS

In this work, we have developed an efficient strategy for identifying mutations that impact receptor function by significantly impeding the gating pathway. The method involves combining mutations of extracellular domain residues proposed to be functionally important with a known gating pathway (reporter) mutation. For interesting sites, ELFCAR can provide guidance for more focused, advanced studies, such as detailed unnatural amino acid mutagenesis of putative binding residues or single-channel analysis, where possible, for gating residues.

The kinetic model of Scheme 1 refers to the nAChR, but it contains the essential features of any allosteric system. There is a binding interaction with an allosteric effector and an

intrinsic conformational change associated with the signaling event. The former is a bimolecular association, and so is saturable at high ligand concentration. However, the conformational change is unimolecular, and so it is an intrinsic property of the system. It is the combination of these two processes that produces the curvature of Fig. 2 and thus allows for the specific application of mutant cycle analysis presented here. As such, we anticipate that the same approach could be applied to other allosteric systems, allowing a facile means to identify the roles of particular residues in a complex protein system. Thus, although this study has focused on a single Cys-loop receptor, we believe the approach is broadly applicable to other Cys-loop receptors and to allosteric receptors in general. Certainly, comparable reporter residues can be found in the other Cys-loop receptors; the L9′ residue is highly conserved and it seems likely to play an important gating role throughout the family. We emphasize that, although all members of the Cys-loop family are genetic orthologs, functional paralogs, and structural homologs, there is growing evidence that the detailed mechanisms of action will vary from system to system (41). Thus, this approach, based on the readily obtained EC_{50} measure, offers a robust and efficient way to search for such variations in gating mechanism.

SUPPORTING MATERIAL

Three figures and supporting text are available at http://www.biophysj.org/biophysj/supplemental/S0006-3495(09)00477-9.

We thank B. N. Cohen for advice on single-channel recording and analysis.

This work was supported by the National Institutes of Health (NS 34407; NS 11756). J.A.P.S. was partially supported by a National Research Service Award training grant. K.R.G. was partially supported by a National Science Foundation Graduate Research Fellowship.

REFERENCES

1. Connolly, C. N., and K. A. Wafford. 2004. The Cys-loop superfamily of ligand-gated ion channels: the impact of receptor structure on function. *Biochem. Soc. Trans.* 32:529–534.
2. Grutter, T., and J. P. Changeux. 2001. Nicotinic receptors in wonderland. *Trends Biochem. Sci.* 26:459–463.
3. Lester, H. A., M. I. Dibas, D. S. Dahan, J. F. Leite, and D. A. Dougherty. 2004. Cys-loop receptors: new twists and turns. *Trends Neurosci.* 27:329–336.
4. Sine, S. M., and A. G. Engel. 2006. Recent advances in Cys-loop receptor structure and function. *Nature*. 440:448–455.
5. Changeux, J. P., and S. J. Edelstein. 2005. Allosteric mechanisms of signal transduction. *Science*. 308:1424–1428.
6. Sixma, T. K., and A. B. Smit. 2003. Acetylcholine binding protein (AChBP): a secreted glial protein that provides a high-resolution model for the extracellular domain of pentameric ligand-gated ion channels. *Annu. Rev. Biophys. Biomol. Struct.* 32:311–334.
7. Unwin, N. 2005. Refined structure of the nicotinic acetylcholine receptor at 4 angstrom resolution. *J. Mol. Biol.* 346:967–989.
8. Peters, J. A., T. G. Hales, and J. J. Lambert. 2005. Molecular determinants of single-channel conductance and ion selectivity in the Cys-loop family: insights from the 5–HT3 receptor. *Trends Pharmacol. Sci.* 26:587–594.
9. Chang, Y., and D. S. Weiss. 1999. Channel opening locks agonist onto the GABAC receptor. *Nat. Neurosci.* 2:219–225.
10. Davies, P. A., M. Pistis, M. C. Hanna, J. A. Peters, J. J. Lambert, et al. 1999. The 5–HT3B subunit is a major determinant of serotonin-receptor function. *Nature*. 397:359–363.
11. Keramidas, A., and N. L. Harrison. 2008. Agonist-dependent single channel current and gating in alpha4beta2delta and alpha1beta2gamma2S GABAA receptors. *J. Gen. Physiol.* 131:163–181.
12. Legendre, P. 2001. The glycinergic inhibitory synapse. *Cell. Mol. Life Sci.* 58:760–793.
13. Li, G., and L. Niu. 2004. How fast does the G1uR1Q(flip) channel open? *J. Biol. Chem.* 279:3990–3997.
14. Nowak, M. W., J. P. Gallivan, S. K. Silverman, C. G. Labarca, D. A. Dougherty, et al. 1998. *In vivo* incorporation of unnatural amino acids into ion channels in a *Xenopus* oocyte expression system. *Methods Enzymol.* 293:504–529.
15. Hamill, O. P., A. Marty, E. Neher, B. Sakmann, and F. J. Sigworth. 1981. Improved patch-clamp techniques for high resolution current recording from cells and cell-free membrane patches. *Pflugers Arch.* 391:85–100.
16. Filatov, G. N., and M. M. White. 1995. The role of conserved leucines in the M2 domain of the acetylcholine receptor in channel gating. *Mol. Pharmacol.* 48:379–384.
17. Labarca, C., M. W. Nowak, H. Zhang, L. Tang, P. Deshpande, et al. 1995. Channel gating governed symmetrically by conserved leucine residues in the M2 domain of nicotinic receptors. *Nature*. 376:514–516.
18. Kalbaugh, T. L. 2004. Ligand-binding residues integrate affinity and efficacy in the NMDA receptor. *Mol. Pharmacol.* 66:209–219.
19. Edelstein, S. J., O. Schaad, and J. P. Changeux. 1997. Single binding versus single channel recordings: a new approach to study ionotropic receptors. *Biochemistry*. 36:13755–13760.
20. Mitra, A., G. D. Cymes, and A. Auerbach. 2005. Dynamics of the acetylcholine receptor pore at the gating transition state. *Proc. Natl. Acad. Sci. USA*. 102:15069–15074.
21. Kosolapov, A. V., G. N. Filatov, and M. M. White. 2000. Acetylcholine receptor gating is influenced by the polarity of amino acids at position 9′ in the M2 domain. *J. Membr. Biol.* 174:191–197.
22. Sigurdson, W., J. Chen, M. Akabas, A. Karlin, and A. Auerbach. 1994. Single-channel kinetic-analysis of mouse Achr M2 mutants alpha-L251c and alpha-S248c. *Biophys. J.* 66, A212–A212. (Abstr.)
23. Kearney, P. C., M. W. Nowak, W. Zhong, S. K. Silverman, H. A. Lester, et al. 1996. Dose-response relations for unnatural amino acids at the agonist binding site of the nicotinic acetylcholine receptor: tests with novel side chains and with several agonists. *Mol. Pharmacol.* 50:1401–1412.
24. Zhong, W., J. P. Gallivan, Y. Zhang, L. Li, H. A. Lester, et al. 1998. From ab initio quantum mechanics to molecular neurobiology: a cation-pi binding site in the nicotinic receptor. *Proc. Natl. Acad. Sci. USA*. 95:12088–12093.
25. Akk, G., S. Sine, and A. Auerbach. 1996. Binding sites contribute unequally to the gating of mouse nicotinic alpha D200N acetylcholine receptors. *J. Physiol.* 496:185–196.
26. Akk, G., M. Zhou, and A. Auerbach. 1999. A mutational analysis of the acetylcholine receptor channel transmitter binding site. *Biophys. J.* 76:207–218.
27. Chen, J., Y. Zhang, G. Akk, S. Sine, and A. Auerbach. 1995. Activation kinetics of recombinant mouse nicotinic acetylcholine receptors: mutations of alpha-subunit tyrosine 190 affect both binding and gating. *Biophys. J.* 69:849–859.
28. Mukhtasimova, N., C. Free, and S. M. Sine. 2005. Initial coupling of binding to gating mediated by conserved residues in the muscle nicotinic receptor. *J. Gen. Physiol.* 126:23–39.
29. O'Leary, M. E., and M. M. White. 1992. Mutational analysis of ligand-induced activation of the Torpedo acetylcholine receptor. *J. Biol. Chem.* 267:8360–8365.

30. Sine, S. M., X. M. Shen, H. L. Wang, K. Ohno, W. Y. Lee, et al. 2002. Naturally occurring mutations at the acetylcholine receptor binding site independently alter ACh binding and channel gating. *J. Gen. Physiol.* 120:483–496.

31. Xie, Y., and J. B. Cohen. 2001. Contributions of Torpedo nicotinic acetylcholine receptor gamma Trp-55 and delta Trp-57 to agonist and competitive antagonist function. *J. Biol. Chem.* 276:2417–2426.

32. Chapman, E., J. S. Thorson, and P. G. Schultz. 1997. Mutational analysis of backbone hydrogen bonds in Staphylococcal nuclease. *J. Am. Chem. Soc.* 119:7151–7152.

33. England, P. M., Y. Zhang, D. A. Dougherty, and H. A. Lester. 1999. Backbone mutations in transmembrane domains of a ligand-gated ion channel: implications for the mechanism of gating. *Cell.* 96:89–98.

34. Kash, T. L., A. Jenkins, J. C. Kelley, J. R. Trudell, and N. L. Harrison. 2003. Coupling of agonist binding to channel gating in the GABA(A) receptor. *Nature.* 421:272–275.

35. Price, K. L., K. S. Millen, and S. C. Lummis. 2007. Transducing agonist binding to channel gating involves different interactions in 5–HT3 and GABAC receptors. *J. Biol. Chem.* 282:25623–25630.

36. Venkatachalan, S. P., and C. Czajkowski. 2008. A conserved salt bridge critical for GABAA receptor function and loop C dynamics. *Proc. Natl. Acad. Sci. USA.* 105:13604–13609.

37. Xiu, X., A. P. Hanek, J. Wang, H. A. Lester, and D. A. Dougherty. 2005. A unified view of the role of electrostatic interactions in modulating the gating of Cys loop receptors. *J. Biol. Chem.* 280:41655–41666.

38. Brejc, K., W. J. van Dijk, R. V. Klaassen, M. Schuurmans, J. van Der Oost, et al. 2001. Crystal structure of an ACh-binding protein reveals the ligand-binding domain of nicotinic receptors. *Nature.* 411:269–276.

39. Corringer, P. J., N. Le Novere, and J. P. Changeux. 2000. Nicotinic receptors at the amino acid level. *Annu. Rev. Pharmacol. Toxicol.* 40:431–458.

40. Dougherty, D. A., and D. A. Stauffer. 1990. Acetylcholine binding by a synthetic receptor. Implications for biological recognition. *Science.* 250:1558–1560.

41. Dougherty, D. A. 2008. Cys-loop neuroreceptors: structure to the rescue? *Chem. Rev.* 108:1642–1653.

42. Beene, D. L., G. S. Brandt, W. G. Zhong, N. M. Zacharias, H. A. Lester, et al. 2002. Cation-pi interactions in ligand recognition by serotonergic (5–HT3A) and nicotinic acetylcholine receptors: The anomalous binding properties of nicotine. *Biochemistry.* 41:10262–10269.

43. Akk, G. 2001. Aromatics at the murine nicotinic receptor agonist binding site: mutational analysis of the alphaY93 and alphaW149 residues. *J. Physiol.* 535:729–740.

44. Mu, T. W., H. A. Lester, and D. A. Dougherty. 2003. Different binding orientations for the same agonist at homologous receptors: a lock and key or a simple wedge? *J. Am. Chem. Soc.* 125:6850–6851.

45. Kearney, P. C., H. Zhang, W. Zhong, D. A. Dougherty, and H. A. Lester. 1996. Determinants of nicotinic receptor gating in natural and unnatural side chain structures at the M2 9′ position. *Neuron.* 17:1221–1229.

46. Padgett, C. L., A. P. Hanek, H. A. Lester, D. A. Dougherty, and S. C. R. Lummis. 2007. Unnatural amino acid mutagenesis of the GABA(A) receptor binding site residues reveals a novel cation-pi interaction between GABA and beta(2)Tyr97. *J. Neurosci.* 27:886–892.

47. Gleitsman, K. R., S. M. A. Kedrowski, H. A. Lester, and D. A. Dougherty. 2008. An intersubunit hydrogen bond in the nicotinic acetylcholine receptor that contributes to channel gating. *J. Biol. Chem.* 283:35638–35643.

48. Gao, F., N. Bren, T. P. Burghardt, S. Hansen, R. H. Henchman, et al. 2005. Agonist-mediated conformational changes in acetylcholine-binding protein revealed by simulation and intrinsic tryptophan fluorescence. *J. Biol. Chem.* 280:8443–8451.

49. Miyazawa, A., Y. Fujiyoshi, and N. Unwin. 2003. Structure and gating mechanism of the acetylcholine receptor pore. *Nature.* 423:949–955.

50. Akk, G. 2002. Contributions of the non-alpha subunit residues (loop D) to agonist binding and channel gating in the muscle nicotinic acetylcholine receptor. *J. Physiol.* 544:695–705.

51. Cashin, A. L., E. J. Petersson, H. A. Lester, and D. A. Dougherty. 2005. Using physical chemistry to differentiate nicotinic from cholinergic agonists at the nicotinic acetylcholine receptor. *J. Am. Chem. Soc.* 127:350–356.